Validation Experiment Design of a PMU–Based Application for Detection of Sub-Synchronous Oscillations

José Luis Domínguez-García*, Maxime Baudette†, Gerard Del-Rosario*, Albert Ruíz-Alvárez*,
Muhammad Shoaib Almas†, Ignasi Cairó* and Luigi Vanfretti†‡.
*Catalonia Institute for Energy Research, Barcelona, Spain.
†Electric Power Systems Department, KTH Royal Institute of Technology, Stockholm, Sweden.
‡Research and Development Division, Statnett SF, Oslo, Norway.

***Abstract*—This paper presents an approach to design laboratory experiments able to test the functional performance of a PMU-based application. The function of this application is to detect sub-synchronous oscillatory dynamics product of wind farm-to-grid interactions.**

The designed experiments are carried out in operation conditions similar to those that the PMU-based application would experience in field implementations, while the approach adopted for experiment design takes into account technical limitations of laboratory equipment.

The experiments are performed in a laboratory which has been equipped with synchrophasor technology for the purposes of this work. Real PMU devices physically connected on a small replica of a three-phase low voltage micro-grid where oscillations can be systematically injected.

***Index Terms*—Low Frequency Oscillations, Monitoring, Oscillation Detection, Phasor Measurement Units, Wind Power, Laboratory characterization**

I. Introduction

The penetration of distributed renewable generation sources within both distribution and transmission grids is rapidly increasing [1]. Consequently, the power delivery infrastructure is experiencing a transition towards high reliance on renewable energy sources such as wind and sun. Such generation systems present high variability, intermittence and uncertainty. The inclusion of these technologies and their interaction with other elements of the transmission and distribution network may result in stability issues, and power quality degradation [2].

Considering the example of wind power and its large penetration in the production share, its impact on power system dynamics is a relevant issue for transmission system operators (TSOs) [3], [4]. For the sake of illustration, consider the case of sub-synchronous oscillation phenomena in the USA after the analysis of archived measurements from several PMUs installed in their power system [5]. In this example sub-synchronous oscillations (including low frequency oscillations, sub–synchronous resonances, flicker, etc.) appear across the system at frequencies ranging from 0.1 up to about 40 Hz, depending on the oscillatory dynamics being excited [4].

PMU devices provide GPS time-stamped synchronized data at high reporting rates. Hence, the use of PMUs could provide new means to detect stability and power quality issues in power networks across different voltage levels. To this end, new PMU-based software applications are required. These new tools can help providing operators with better information about undesired system dynamics. However, their development is subjected to the access to relevant PMU data [6].

In this paper, a generic laboratory equipment validation approach through device characterization using simple metrics is proposed. This approach aims to reduce testing costs by avoiding the need of purchasing new dedicated laboratory equipment. The paper shows that proper validation of PMU-based applications requires an analysis of the technical limitations of a validation environment, and it demonstrates how to quantify the impact of the environment by assessing the performance of the hardware and software involved.

II. Experimental Set-up

The implemented laboratory is a flexible testing system representing a small replica of a three-phase micro-grid. It encompasses emulated, semi-emulated (i.e. wind turbine test-benches), and real power system components (such as storage devices). The energy management system of the micro-grid complies with the IEC 61850 standard [7], however it did not provide facilities to deploy PMU applications.

A. Emulators

Emulators are flexible power electronics-based units that can generate variable active and reactive power. Active and reactive power are independently controlled, limited only by the maximum apparent power (5 kVA). Emulators can be configured to behave as any renewable energy source, batteries, variable loads, electric vehicle (EV) chargers, etc. through the definition of the desired power profiles [7].

An emulator is composed of two identical three-phase AC/DC converters in back-to-back configuration, allowing bidirectional power flow. One converter is referred to as Active

978-1-4799-7993-6/15/$31.00 ©2015 IEEE

Rectifier (AR) and the other one is referred to as Active Front End (AFE). The former controls the DC bus voltage to keep it within a stable range. The latter receives three-phase active power and reactive power reference values (P^* and Q^*, respectively) and tracks them.

B. Phasor Measurement Units (PMU)

Two of the emulators are equipped with PMUs, which measure three-phase voltages and currents from the Active Front End. The PMUs used for the experiment are based on the National Instruments CompactRIO platform, shown in Fig. 1. The software inside this device is compliant with the IEEE C37.118-2005 Standard for Synchrophasors for Power Systems [8]. Each PMU is composed of NI cRIO-9074 (real-time acquisition and processing chassis), NI 9225 (Three-phase low voltage analog input), NI 9227 (Three-phase 5A current analog input) and NI 9467 (GPS antenna input).

The voltage input module is connected directly to the three-phase voltage from the AFE of the emulator. The current input modules channels are not connected directly to the power circuit; current transformers [9] are used to adapt current magnitudes to the maximum current allowed by each channel.

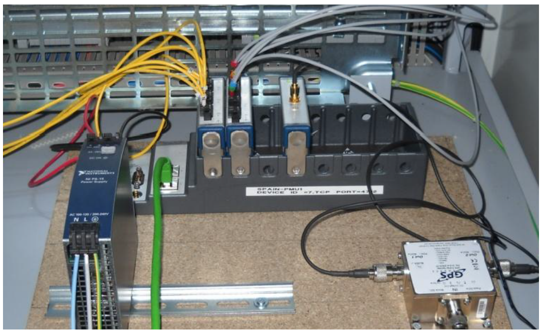

Fig. 1. cRIO 9074 PMU connected to the emulator.

C. Phasor Data Concentrator (PDC) and IEEE C37.118.2 Data Acquisition

A PDC was installed in a computer at the laboratory, and configured to receive measurements from the PMUs installed at the emulators. The PDC time-aligns and concentrates the data for archiving or forwarding to another client.

For testing the monitoring application, the PDC was configured to deliver the measurements to the application during different experiments. The ability of the tool to receive measurements using the IEEE C37.118.2 protocol is provided by the use of Statnett's Synchrophasor SDK (S^3DK)[10], which is a real-time data mediator for LabVIEW.

S^3DK receives the phasor data and parses the IEEE C37.118.2 protocol. The same software provides the measurements to the LabVIEW environment, where the monitoring tool was implemented [11].

D. GPS Antenna Installation

A GPS antenna [12] was installed on the roof of the facility to ensure good GPS signal reception. The PMUs were installed in the basement of the building (i.e. 20 meters away from the antenna). Thus, it was necessary to install an additional low-noise amplifier [13] to compensate for cable losses and obtain an acceptable Signal to Noise Ratio (SNR).

Figure 2 presents a general scheme of the complete setup.

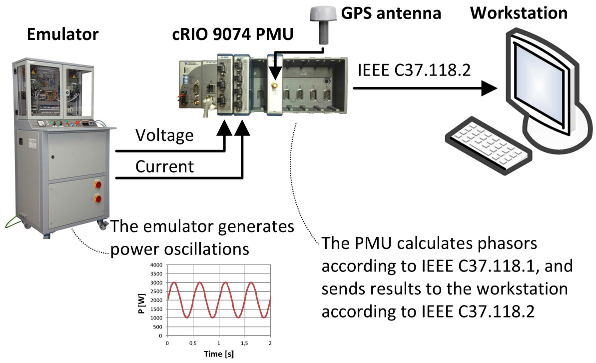

Fig. 2. Laboratory set-up scheme showing equipment used.

III. Design of Validation Experiments considering Equipment Constraints

Ideally, one should know a priori the technical limitations of both the hardware and software used in a laboratory in order to design validation experiments, and design constraints for each specific study case. However, if a laboratory is originally designed for different purposes other than those required for the specific validation experiments, it is necessary to explore the capabilities of existing laboratory devices, and determine their potential limitations. When this is the case, the adequacy of the equipment for such studies must be ensured so to provide reliable results. This Section proposes a general and simple approach for probing technical limitations of a laboratory and designing experiments accordingly, this is illustrated using the implemented microgrid as test case.

A. Generation and Transmission of Designed Signals

As mentioned in Section II-A, the emulators track the P^* reference value for their power output, with a specific dynamic governed by the emulators' controller. Thus, active power profiles can be generated by the emulators, providing P^* reference values according the desired profile. The approach adopted to provide reference values to the emulator requires dedicated computer software and a direct communication link with an emulator.

The computer software generates the P^* reference values as periodical samples of the desired profile and sends them periodically to the AFE via CAN bus (see Fig. 3). The time between two messages by design is expected to be uniform and equal to 16 milliseconds (i.e. $\Delta t = 16ms$).

Since the main idea of the experiment is to validate sub–synchronous oscillations, a simple sinusoidal profile was adopted.

$$P^*(t) = P_{const} + P_{ampl} \sin(2\pi f_{osc} t) \quad (1)$$

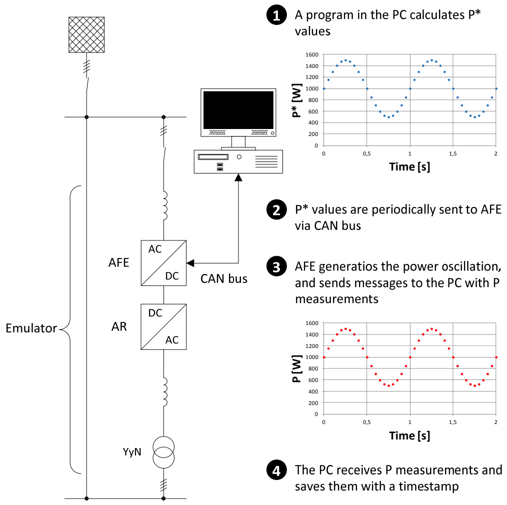

Fig. 3. Set-up for power oscillations generation.

Note that in (1), $P^*(t)$ is not instantaneous power (i.e. it is not $p(t) = v(t) \cdot i(t)$), but variable three-phase power. P_{const} is the predefined average active power, P_{ampl} represents the amplitude of the oscillating power injected and f_{osc} is the frequency of the power oscillation.

It is worth mentioning that the use of more realistic power profiles do not provide better insight of the detection tool validity, since the tool filters the input signal frequencies by using various band-pass filters with different frequency ranges.

B. Limitations

As the experimental set-up involved real power system components and a set of in-house software tools for controlling them, limitations were to be expected. As such, the primary limitation is given by the nominal power of the emulators, that is 5 kVA. Additionally the strategy adopted to generate different types of power oscillations was to periodically send new P^* reference values to the emulator. This was affected by non-deterministic communication delays, as shown on Fig. 4. In this figure it can be seen that the time among messages Δt (which was expected to be constant and uniform) varies in the range of 15-16 ms. Moreover, it must be noticed that the time measured is rounded by the PC used to a millisecond precision. This random variability could slightly affect the emulator's dynamic response and precision.

Initially, preliminary testing of the emulators showed poor dynamic performance for frequencies above 1 Hz due to their very slow dynamic response. This was due to the fact that the emulators were originally designed for high level energy management system integration, and considered only smooth responses with long time interval between messages. To address this issue, the PI controllers of the AFE were calibrated. Figure 5 shows the step responses of one emulator before and after the re-tuning of the PI controllers. The new response is much faster, enabling the cabinet to generate higher frequency power oscillations.

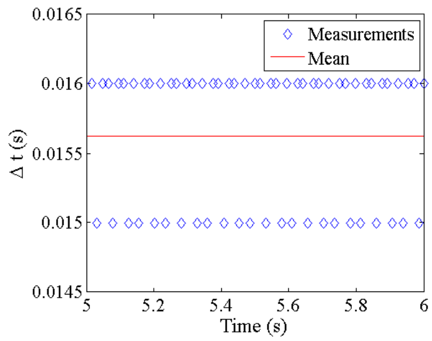

Fig. 4. Time between two messages (Δt) on the CAN bus with variable communication delay

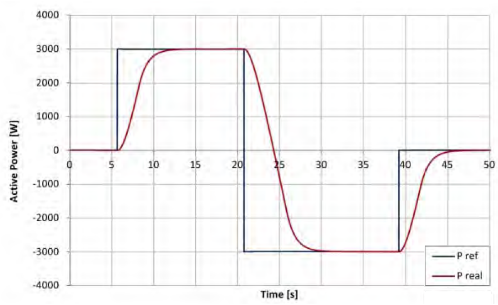

(a)

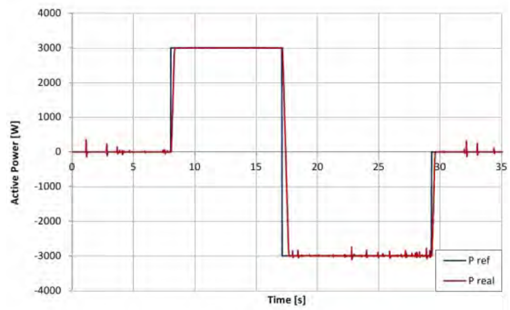

(b)

Fig. 5. Comparison of the step response of one emulator before (a) and after (b) calibrating the PI controllers

The dynamic response of the newly tuned PI-controls of the emulators was tested with a set of fixed-frequency power oscillations profiles, as shown in Fig. 6. In these graphs, blue lines correspond to P^* values (being set P_{const} and P_{ampl} as 2000 and 1000 W, respectively), and red lines correspond to P_{real} measurements calculated by the AFE and sent to the PC. It shows that at 6 Hz the emulator experiences difficulties to reproduce the reference signal, demonstrating a potential upper bound limitation on frequency resolution required for testing the application. The dynamic performances of the emulators will be assessed in more detail next.

1) Equipment characterization: As previously stated to validate the performances of the sub–synchronous oscillation detection tool, it is important to assess the performances of the emulators, which may affect the results of the application.

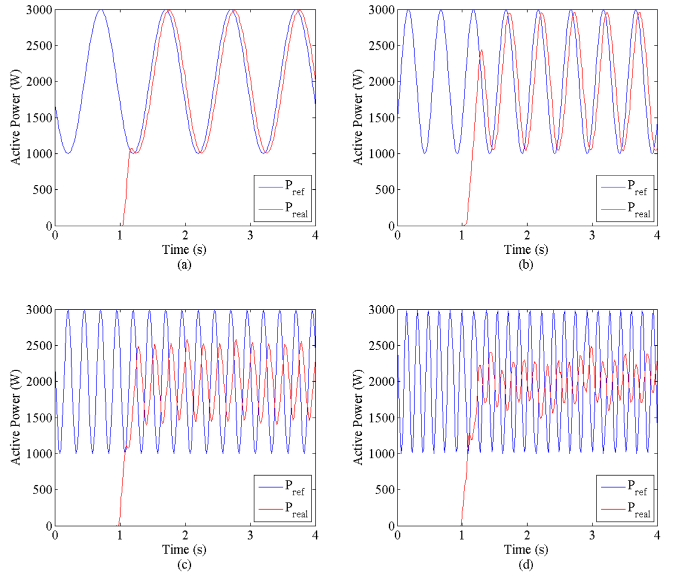

Fig. 6. Power oscillations at different frequencies: (a) 1 Hz, (b) 2 Hz, (c) 4 Hz, (d) 6 Hz.

Several experiments have been carried out with the emulators to generate power oscillations with different frequencies (f_{osc}) in the range of $[0.14\ 14\ Hz]$.

The range of validity of the experiments, designed when subject to technical constraints, is assessed by providing response metrics. These metrics consider mainly the use of a simple known reference signal (i.e. frequency and amplitude), and comparing it with the measured response of the emulators. From these experiments a behavioral curve of the equipment can be estimated. This defines the lab equipment characteristics, which can be used to determine the range where the equipment is capable to perform properly for desired experimental tests.

The results obtained from this wide range of tests are used to characterize the emulator dynamics, allowing quantifying frequency generation limits and the potential P_{amp} decay from the set value. The measures used for this analysis are taken from the AFE DSP output which is connected directly to the PC.

Figure 7 summarizes the results of the analysis, where it can be noticed that the higher the frequency generated, the less precise the emulators are producing the desired output. In particular, Fig. 7(a) shows a characteristic to that of a low-pass filter, where the amplitude reproduced drops down to 50% at around $4\ Hz$. The obtained amplitude is 100% for oscillations at $1\ Hz$, and 30% for oscillations at $6\ Hz$. It must be also noted that at oscillation frequencies of $10\ Hz$, the expected amplitude will be below 10% of the references value.

Figure 7(b) shows the difference between the generated frequency and the reference frequency over the reference value. Disregarding outliers, the error increases linearly with the increase of the reference frequency.

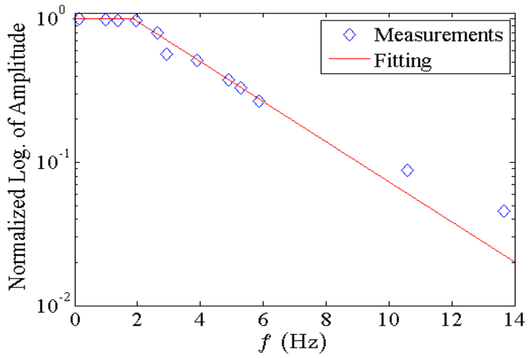

(a) Amplitude tracking performance

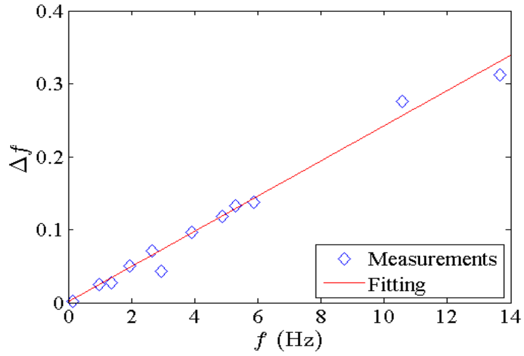

(b) Frequency tracking performance

Fig. 7. Analysis of the performances of the response of the emulators

C. Design of Experiments

The original desired profile for the power output of the emulators was formulated in 1. Taking into account the known limitations and using the characteristic behavior obtained in the previous subsections, the resulting power profile can be defined.

From the characteristic graph, it is possible to determine frequency validity boundaries. Here Δf is defined to be 0.15 implying a maximum f_{osc} of $6\ Hz$. Thus, frequencies above 6 Hz and up to 25 Hz were not considered. The amplitude decay for the worst case included in the study was 30% of the value set (P_{ampl}).

Then, the oscillation experimental power profile can be defined by considering the following constraints:

$$P_{const} + P_{ampl} \leq 5000\text{VA}, \tag{2}$$

$$f_{osc} \in [0\ 6\text{Hz}]. \tag{3}$$

Combining (1) - (3) gives the general form of the design of experiments to test the application:

$$\begin{aligned} &P^*(t) = P_{const} + P_{ampl} \sin(2\pi f_{osc} t) \\ &\text{subject to} \\ &P_{const} + P_{ampl} \leq 5000 \text{ VA} \\ &0 \leq f_{osc} \leq 6 \text{ Hz.} \end{aligned}$$

IV. Validation Experiments of Power Oscillation Detection Tools

Next, a PMU-based monitoring tool, designed to detect oscillations in the power grid, is experimentally validated in the laboratory presented in Section II and compared with a conventional power analyzer. The validation experiments presented here are a representative sub-set of the whole potential experiments discussed in Section III-C considering a very low frequency (well emulated) and one close to equipment limits. Two different types of sub-synchronous frequency oscillations which may occur in power systems serve as illustration : Local oscillation modes (1 Hz) and control, flicker or sub-synchronous resonance modes (6 Hz) [14], [5]. It must be noted that the oscillations are injected by an emulator - they are not obtained naturally by system dynamics.

A. Case 1: Local oscillation mode test

In the first case, the monitoring of local oscillatory modes (1 Hz in this example) by the developed PMU application is experimentally validated through the injection of a power profile:

$$P^*(t) = 2000 + 1000\sin(2\pi t).$$

Figure 8 shows the generated signals, where the blue signal corresponds to P^* and the red signal corresponds to P_{real} measurements from the AFE.

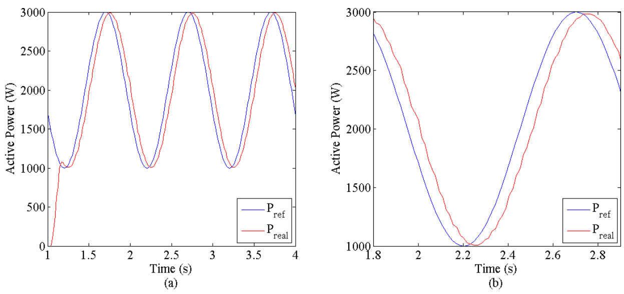

Fig. 8. 1 Hz power oscillation. (b) is an enlargement of (a).

Figure 9 shows screenshot of the measurements made by the existing conventional power analyzer in the lab. It can be noticed that, for the 1 Hz power oscillation case, the frequency can be properly observed. However, it is worth noting that no FFT is performed, thus requiring of offline post–processing for frequency detection.

A screenshot of one of the modules (energy and frequency estimation) of the PMU-based software tool is shown in Fig. 10. Note that since the oscillation is kept constant, the resulting energy calculation is almost constant once the low frequency oscillation is detected. It can also be seen in the graphical display that the severity of the fault is flagged as "*Danger*", since the amplitude of the oscillation has gone beyond the configured threshold [15]. Figure 10 shows an estimated frequency around 1.1 Hz. The difference with the reference signal can be explained by Section III-C.

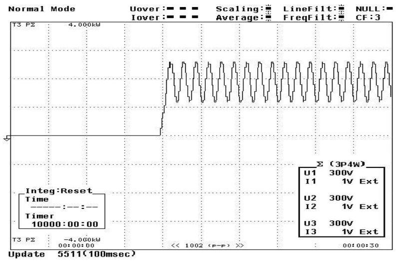

Fig. 9. Power measured by a Yokogawa power analyser for a 1 Hz frequency power oscillation (3 seconds horizontal and 1000W vertical per interval).

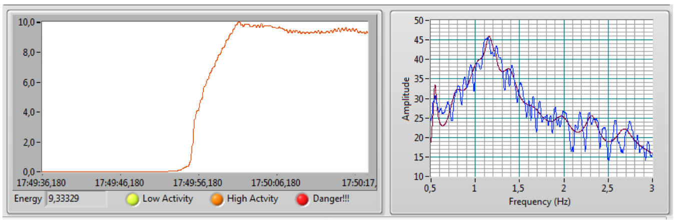

Fig. 10. Oscillation detection and Frequency measured by the PMU application.

B. Case 2: Sub-synchronous oscillation test

In the second case, the injected oscillation is in the range of sub-synchronous oscillations as experienced in Oklahoma (6 Hz in this case) [16]. Similarly to the previous case, the power profile injected for testing can be described by

$$P^*(t) = 2000 + 1000\sin(2\pi \cdot 6t).$$

Figure 11 shows the oscillation generated, and it can be observed that P_{real} is reduced by 70%, which was explained in the previous Section.

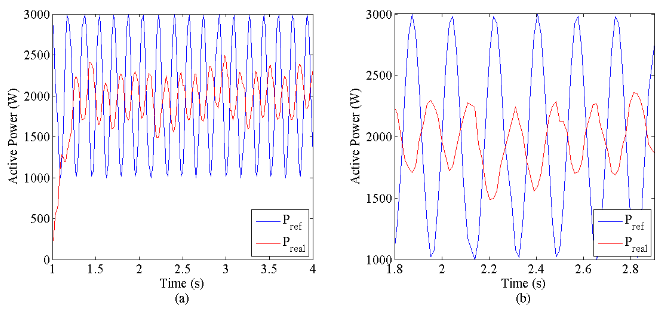

Fig. 11. 6 Hz power oscillation. (b) is an enlargement of (a).

Again Figure 12 shows screenshots of the signals detected by the power analyzer when injecting 6 Hz power oscillations. It can be stated that such equipment is not well-suited to the analysis of higher frequency dynamic phenomena due to low frequency sampling.

As in the previous case, a screenshot of the monitoring tool is shown in Fig. 13. The energy computed by the tool is also constant, as the oscillation injection is kept constant, but of lower magnitude, which is due to the lower amplitude of the oscillation generated by the converters. As it can be seen,

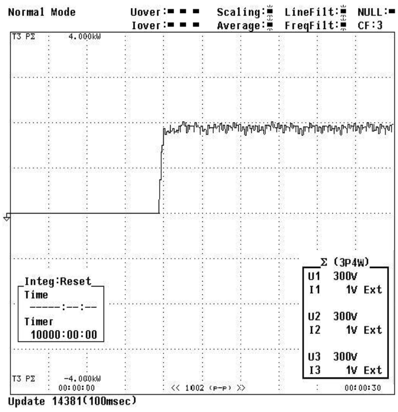

Fig. 12. Power measured by a Yokogawa power analyser for a 6 Hz frequency power oscillation (3 seconds horizontal and 1000W vertical per interval).

there is an energy decay of about 70 % in comparison with 1 Hz case, as it was predicted by the experiment validation metrics. This results in a phenomenon flagged with a severity of "*Low activity*". The frequency estimate has lower resolution as the converter has difficulties with signal reconstruction. This is shown in Fig 13, where the oscillation frequency is estimated slightly above 6.1 Hz. This result correlates the study performed in the previous Section.

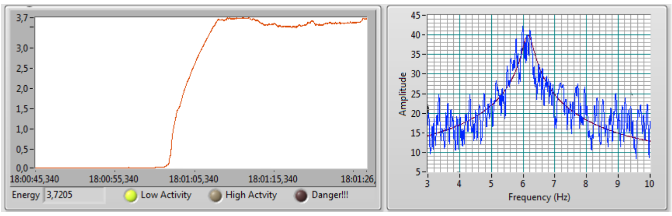

Fig. 13. Oscillation detection and Frequency measured by the PMU application tool.

This case demonstrates, the ability of the tool to detect low frequency oscillations faster than those in the previous case, i.e., oscillation detection is possible at arbitrary frequencies below the Nyquist limit of the PMU reporting rate used.

V. Conclusion

Experimental validation of a PMU-based monitoring application tool developed for fast detection of sub-synchronous wind farm oscillations has been carried out within this paper. The real devices used and their adaptation for experimental validation have been presented, as well as the technical limitations that need to be taken into account for validation experiment design.

For proper validation of a PMU application, technical limitations need to be analyzed prior to the design of validation experiments. An important contribution of this paper has been to demonstrate how to quantify the impact of a laboratory set up by assessing the performance of the hardware and software used within an experiment.

The most important conclusion from this work is that there is a need to establish a framework for experiment design for strict testing and validation of synchrophasor applications. Such framework will provide a greater confidence in the methods and results from PMU applications, as well as allowing to identify potential pitfalls and limitations that need to be redesigned prior to PMU application deployment.

Acknowledgment

The economical support of the institutions and funding bodies listed below is sincerely acknowledged:

- EIT KIC InnoEnergy through Action 2.6 of the Smart Power project.
- Nordic Energy Research for the STRONg^2*rid* project.
- Statnett SF, the Norwegian TSO.
- STandUP *for* Energy collaboration initiative.
- The EU funded FP7 Ideal grid for all (IDE4L) project with the grant number 608860.

References

[1] Wilkes J. and J. Moccia, "Wind in power: 2012 European statistics," EWEA, Tech. Rep., 2013.

[2] S. Chowdhury and P. Crossley, *Microgrids and active distribution networks*, iet renewa ed. The Institution of Engineering and Technology, 2009.

[3] ENTSO-E, "ENTSO-E Network Code for Requirements for Grid Connection Applicable to all Generators," 2013.

[4] J. L. Domínguez-García, O. Gomis-Bellmunt, F. D. Bianchi, and A. Sumper, "Power oscillation damping supported by wind power: A review," *Renew. Sustain. Energy Rev.*, vol. 16, no. 7, pp. 4994–5006, Sep. 2012.

[5] Y. H. Wan, "Synchronized Phasor Data for Analyzing Wind Power Plant Dynamic Behaviour and Model Validation," NREL, Tech. Rep., 2013.

[6] D. M. Laverty, R. J. Best, P. Brogan, I. Al Khatib, L. Vanfretti, and D. J. Morrow, "The OpenPMU platform for open-source phasor measurements," *IEEE Trans. Instrum. Meas.*, vol. 62, no. 4, pp. 701–709, Apr. 2013.

[7] A. Ruiz-Álvarez, A. Colet-Subirachs, F. Álvarez-Cuevas Figuerola, O. Gomis-Bellmunt, and A. Sudrià-Andreu, "Operation of a utility connected microgrid using an IEC 61850-based multi-level management system," *IEEE Trans. Smart Grid*, vol. 3, no. 2, pp. 858–865, Jun. 2012.

[8] IEEE, "IEEE Standard for Synchrophasor Data Transfer for Power Systems," *IEEE Std C37.118.2-2011 (Revision IEEE Std C37.118-2005)*, pp. 1–53, 2011.

[9] "Current transformers TM45, Circuitor." [Online]. Available: http://circutor.com/docs/FT_M7_TM45_EN.pdf

[10] L. Vanfretti, V. H. Aarstrand, M. S. Almas, V. S. Peric, and J. O. Gjerde, "A software development toolkit for real-time synchrophasor applications," in *2013 IEEE Grenoble Conf.* IEEE, 2013, pp. 1–6.

[11] L. Vanfretti, M. Baudette, J. L. Dominguez-Garcia, A. White, M. S. Almas, and J. O. Gjerde, "A pmu-based fast real-time sub-synchronous oscillation detection application," in *15th IEEE International Conference on Environment and Electrical Engineering*, Jun. 2015.

[12] "Bullet GPS Antenna, Trimble." [Online]. Available: http://www.trimble.com/timing/bullet-gps-antenna.aspx

[13] "A11 Amplifier, GPS Source." [Online]. Available: http://www.gpssource.com/products/gps-amplifier/94

[14] M. Klein, G. J. Rogers, and P. Kundur, "A fundamental study of inter-area oscillations in power systems," *IEEE Trans. Power Syst.*, vol. 6, no. 3, pp. 914–921, Aug. 1991.

[15] M. Baudette, L. Vanfretti, G. Del-Rosario, A. Ruíz-Alvarez, J.-L. Domingez, I. Al-Khatib, M. S. Almas, I. Cairo-molins, and J. O. Gjerde, "Validating a Real-Time PMU-Based Application for Monitoring of Sub-Synchronous Wind Farm Oscillations," in *2014 IEEE PES Innovative Smart Grid Technologies Conf., ISGT*, Washington, D.C., Feb. 2014.

[16] A. O. White and S. Chisholm, "Relays Become Problem Solvers," *Transm. Distrib. World*, no. November, pp. 26–33, 2011.